

AD-A102 943 OHIO STATE UNIV COLUMBUS DEPT OF GEODETIC SCIENCE F/6 8/5  
FEASIBILITY STUDIES FOR THE PREDICTION OF THE GRAVITY DISTURBANCE--ETC(U)  
MAR 81 H SUENKEL F19628-79-C-0075

UNCLASSIFIED

DGS-311

AFGL-TR-81-0084

NL

| D+ |  
40 A  
-02 943

END  
DATE PRINTED  
9-81  
OTIC

**LEVEL**

(12)

AFGL-TR-81-0084

43

FEASIBILITY STUDIES FOR THE PREDICTION OF THE  
GRAVITY DISTURBANCE VECTOR IN HIGH ALTITUDES

Hans Sünkel

Department of Geodetic Science  
The Ohio State University  
Research Foundation  
Columbus, Ohio 43210

10

March 1981

DTIC

AUG 1 7 1981

H

Scientific Report No. 5

Approved for public release; distribution unlimited

FILE COPY

AIR FORCE GEOPHYSICS LABORATORY  
AIR FORCE SYSTEMS COMMAND  
UNITED STATES AIR FORCE  
HANSOM AFB, MASSACHUSETTS 01731

81 8 17 056

**Qualified requestors may obtain additional copies from the  
Defense Technical Information Center. All others should  
apply to the National Technical Information Service.**

Unclassified

SECURITY CLASSIFICATION OF THIS PAGE (When Data Entered)

REPORT DOCUMENTATION PAGE		READ INSTRUCTIONS BEFORE COMPLETING FORM
1. REPORT NUMBER AFGL TR-81-0084	2. GOVT ACCESSION NO. AD-A102	3. RECIPIENT'S CATALOG NUMBER 943
4. TITLE (and Subtitle) FEASIBILITY STUDIES FOR THE PREDICTION OF THE GRAVITY DISTURBANCE VECTOR IN HIGH ALTITUDES		5. TYPE OF REPORT & PERIOD COVERED Scientific Report No.5
6. AUTHOR(s) Hans/Sunkel		6. PERFORMING ORG. REPORT NUMBER Report No.311
7. PERFORMING ORGANIZATION NAME AND ADDRESS Department of Geodetic Science The Ohio State University Columbus, Ohio 43210		8. CONTRACT OR GRANT NUMBER(s) F19628-79-C-0075
9. CONTROLLING OFFICE NAME AND ADDRESS Air Force Geophysics Laboratory Hanscom AFB, Massachusetts 01731 Project Monitor - Bela Szabo/LW		10. PROGRAM ELEMENT, PROJECT, TASK AREA & WORK UNIT NUMBERS 62101F 76000BAL
11. MONITORING AGENCY NAME & ADDRESS (if different from Controlling Office)		12. REPORT DATE March 1981
		13. NUMBER OF PAGES 53 pages
		14. SECURITY CLASS. (of this report) Unclassified
		15a. DECLASSIFICATION/DOWNGRADING SCHEDULE
16. DISTRIBUTION STATEMENT (of this Report) Approved for public release; distribution unlimited		
17. DISTRIBUTION STATEMENT (of the abstract entered in Block 20, if different from Report) <i>DTIC</i>		
18. SUPPLEMENTARY NOTES		
19. KEY WORDS (Continue on reverse side if necessary and identify by block number) disturbing potential least-squares collocation integral formula isotropic integral kernel frequency domain		
20. ABSTRACT (Continue on reverse side if necessary and identify by block number) The accuracy of the gravity disturbance vector in high altitude (30,000 - 200,000 feet), predicted from a surface-covering set of mean gravity anomalies, is estimated. Two methods are used and found to provide estimates which differ by less than 10%, the least-squares collocation and the integral solutions for the integral solution, the estimation of the representation error has been performed in the frequency domain. For the collocation solution an optimal algorithm has been developed which takes advantage of:		

the regular data distribution and is up to 64 times faster than a non-optimized solution.

The results indicate that the radial component of the gravity disturbance vector can be estimated with an accuracy of  $\pm 1$  mgal at an altitude of about 50.000 ft on the basis of the available data sets; in order to achieve the same accuracy at 30.000 ft altitude, the data error, particularly that of  $5' \times 5'$  anomalies, has to be reduced by some 60%; the available data distributions are adequate. The prediction error drops quickly with increasing altitude.

The situation is considerably different for the horizontal component: with the best available data distribution an accuracy of  $\pm 2.3$  mgal at 30.000 ft altitude can be achieved; (this corresponds to  $\pm 0.^{\circ}5$  in the direction of the gravity vector.) An accuracy of  $\pm 1$  mgal requires a block size reduction by a factor of 2 not only in the innermost zone, but also up to a spherical distance of about  $30^{\circ}$ ; in addition, the overall data error needs to be reduced by some 30%. The prediction error decreases only slowly with increasing altitude.

Unclassified

## FOREWORD

This report was prepared by Dr. Hans Sünkel, Technical University at Graz, Austria, under Air Force Contract No. F19628-79-C-0075, The Ohio State University Research Foundation, Project No. 711715, Project Supervisor, Urho A. Uotila, Professor, Department of Geodetic Science. The contract covering this research is administered by the Air Force Geophysics Laboratory (AFGL), Hanscom Air Force Base, Massachusetts, with Mr. Bela Szabo, Project Scientist.

Accession For	
WTS: CPW&I	<input checked="" type="checkbox"/>
FILED T.D.	<input type="checkbox"/>
UNCLASSIFIED	<input type="checkbox"/>
SERIALIZED	<input type="checkbox"/>
By _____	
Distribution/	
Availability Codes	
Avail and/or	
DIST : Special	
A	

## C O N T E N T S

1.	Problem formulation	1
2.	The data	2
3.	Collocation solution	5
	3.1 Collocation solution for gridded data	8
4.	Integral approach	16
	4.1 Estimation of the representation error	17
	4.2 Estimation of the error due to data inaccuracy	39
5.	Collocation versus integral approach	41
6.	Results - conclusions	43
	Acknowledgements	50
	Key words	50
	References	51

## 1. PROBLEM FORMULATION

Given a set of mean free air gravity anomalies at sea level and associated rms-error estimates, the accuracy of a predicted gravity disturbance vector in high altitude (30 000 - 200 000 ft) should be estimated. The underlying prediction concept is least-squares collocation based on a homogeneous and isotropic global covariance function for free air gravity anomalies, which is supposed to provide best linear unbiased estimates with "best" depending on the choice of the covariance function and on the data error characteristic.

Although a complete and consistent prediction algorithm (a sub-module of GSPP) was available (Sünkel, 1980), the design of a strictly problem-oriented procedure turned out to be necessary: the prediction algorithm of GSPP is designed for the general case of a heterogeneous set of irregularly distributed data; it does not take advantage of symmetries in the data distribution. Since the data sets to be studied are fairly large (> 2000), a straightforward least-squares collocation solution turned out to be prohibitive because of excessive computation time requirements. Therefore, studies have been carried out which led to the realization of a computer routine, well tailored for the problem in consideration: blockwise homogeneous data which are symmetrically distributed with respect to the computation point. Depending on its latitude, the calculation speed can be increased by a factor of at least 8 and at most 64 relative to non-problem-oriented algorithms. Tests and comparisons with the existing prediction module have been carried out with small data sets.

Stimulated by the result of practical experiments (Rapp and Agajelu, 1975) showing that collocation solutions differ from Poisson integral solutions by about 10 % only, detailed studies were performed using this approach. Rapp's findings are largely confirmed by my results; this is quite remarkable since the integral estimation presented here is almost exclusively performed in the frequency domain.

## 2. THE DATA

The data set to be used in these studies consists of mean free air gravity anomalies covering the surface of the sphere partly as well as totally. The arrangement of the data is symmetrical with respect to the computation point: Starting with  $5' \times 5'$  mean anomalies in a rectangular region with the computation point  $P$  as its center, rectangular zones are defined, each zone being completely covered by mean anomalies,  $15' \times 15'$ ,  $1^\circ \times 1^\circ$  and  $5^\circ \times 5^\circ$  means (Fig. 2.1).

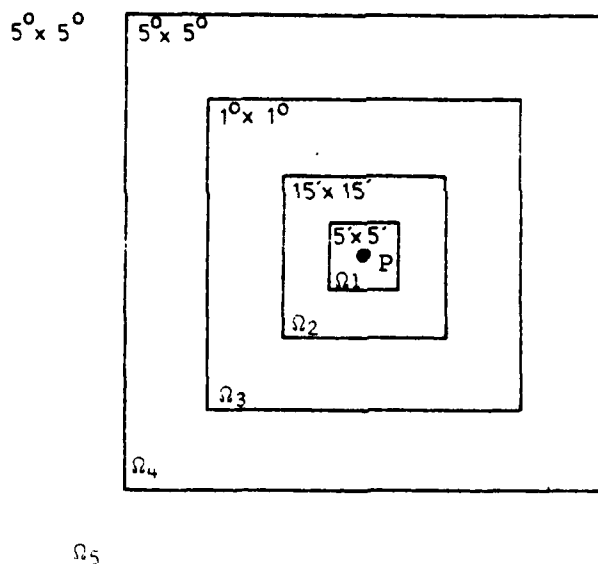


FIG. 2.1 Data arrangement

The prediction (computation) point is assumed to have a latitude of  $\phi_p = 40^\circ$ .

As far as the data distribution and the a priori estimates of corresponding rms-estimates are concerned, 18 cases had to be studied. The following two tables summarize these cases.

Case	$\Omega_1 (5' \times 5')$	$\Omega_2 (15' \times 15')$	$\Omega_3 (1^\circ \times 1^\circ)$	$\Omega_4 (5^\circ \times 5^\circ)$	$\Omega_5 (5^\circ \times 5^\circ)$
1	$2^\circ \times 2^\circ$	$6^\circ \times 8^\circ$	$26^\circ \times 30^\circ$	$50^\circ \times 70^\circ$	$180^\circ \times 360^\circ$
2	$3^\circ \times 4^\circ$	$7^\circ \times 9^\circ$	$26^\circ \times 30^\circ$	$50^\circ \times 70^\circ$	$180^\circ \times 360^\circ$
3	$3^\circ \times 4^\circ$	$7^\circ \times 9^\circ$	$30^\circ \times 34^\circ$	$50^\circ \times 70^\circ$	$180^\circ \times 360^\circ$
4	$3^\circ \times 4^\circ$	$7^\circ \times 9^\circ$	$38^\circ \times 42^\circ$	$50^\circ \times 70^\circ$	$180^\circ \times 360^\circ$
5	$3^\circ \times 4^\circ$	$10^\circ \times 12^\circ$	$26^\circ \times 30^\circ$	$50^\circ \times 70^\circ$	$180^\circ \times 360^\circ$
6	$3^\circ \times 4^\circ$	$16^\circ \times 18^\circ$	$26^\circ \times 30^\circ$	$50^\circ \times 70^\circ$	$180^\circ \times 360^\circ$
7	$7^\circ \times 9^\circ$	$10^\circ \times 12^\circ$	$26^\circ \times 30^\circ$	$50^\circ \times 70^\circ$	$180^\circ \times 360^\circ$
8	$3^\circ \times 4^\circ$	$7^\circ \times 9^\circ$	$26^\circ \times 30^\circ$	$60^\circ \times 100^\circ$	$180^\circ \times 360^\circ$
9	$3^\circ \times 4^\circ$	$16^\circ \times 18^\circ$	$38^\circ \times 42^\circ$	$60^\circ \times 100^\circ$	$180^\circ \times 360^\circ$

TABLE 2.1 Data region sizes ( $\Delta\phi, \Delta\lambda$ ), centered at the computation point.

rms (mgal)	$5' \times 5'$	$15' \times 15'$	$1^\circ \times 1^\circ$	$5^\circ \times 5^\circ (\Omega_4)$	$5^\circ \times 5^\circ (\Omega_5)$
a	$\pm 8$	$\pm 8$	$\pm 5$	$\pm 3$	$\pm 5$
b	$\pm 10$	$\pm 7$	$\pm 4$	$\pm 3$	$\pm 5$

TABLE 2.2 Estimated rms errors of mean anomalies.

Error correlations were to be neglected throughout (data error covariance matrix is diagonal), a questionable assumption in the author's opinion.

Five levels of prediction (= height of the computation point) were considered:

$$h_p = (30\ 000, 40\ 000, 70\ 000, 100\ 000, 200\ 000) \text{ feet.}$$

The estimated quantity is the gravity disturbance vector  $\delta g_p$  which is defined as the difference vector between the actual and the normal gravity vector,

$$\delta g_p = g_p - g_n , \quad (2.1)$$

taken at the same point (Heiskanen and Moritz, 1967, p. 85). The gravity vector is the gradient of the corresponding potential; therefore, the gravity disturbance vector is the gradient of the disturbing potential  $T$ ,

$$\delta g_p = \text{grad}_p T . \quad (2.1)'$$

The following chapters deal with accuracy estimation processes for the 3 components of  $\delta g$ , the radial component  $\delta_r$ , and the two horizontal components  $\delta_\phi$  (along the meridian) and  $\delta_\lambda$  (along the parallel).

### 3. COLLOCATION SOLUTION

The mean square error of a predicted gravity field quantity can be estimated by

$$m_p^2 = C_{pp} - C_p^T \bar{C}^{-1} C_p \quad (3.1)$$

(Moritz, 1980, p.80). Here  $m_p^2$  denotes the predicted mean square error,  $C_{pp}$  the variance of the predicted quantity, and the positive (strictly speaking: non-negative) quantity  $C_p^T \bar{C}^{-1} C_p$  the gain of prediction;  $C_p$  is the cross-covariance vector between the predicted quantity and all data,  $\bar{C} = C + D$ , where  $C$  denotes the data covariance matrix and  $D$  the a priori data error covariance matrix.  $D$  reduces to diagonal form for vanishing error correlations.

All variances and covariances are derived from one common covariance function, say the covariance function of the disturbing potential  $K(P,Q)$ .  $K$  is harmonic with respect to  $P$  and  $Q$  outside some sphere  $r = R_B$ ; furthermore, it is usually chosen to be homogeneous and isotropic, expressed by its independence of horizontal position and direction. This is why  $K(P,Q)$  depends only on the product of the moduli of the radius vectors  $r_R r_Q$  and the spherical distance  $\psi_{PQ}$  between the two points  $P$  and  $Q$  (which are located outside  $r = R_B$ ) ,

$$K(P,Q) = \sum_{n=2}^{\infty} k_n \left( \frac{R_B^2}{r_P r_Q} \right)^{n+1} P_n(\cos \psi_{PQ}) ; \quad (3.2)$$

$\{k_n\}$ ,  $n = 2, \dots$ , denote (model) degree variances and  $P_n$  the  $n$ 'th degree Legendre polynomial.

All covariances (which enter into the estimation equation (3.1)) are obtained by applying the rule of covariance propagation.

Since the linear operator, relating the disturbing potential to the gravity anomaly, is homogeneous and isotropic, the homogeneity and isotropy of the gravity anomaly covariance function follows.

A least-squares collocation solution is burdened by two severe problems: the calculation of the many individual covariances and the inversion of the covariance matrix. Therefore, every possibility to reduce the computational effort should be favorably considered. In the cases to be studied here, it is particularly the regular data distribution which can be advantageously taken into account in the structure of the covariance matrix and its inverse.

The fact that mean anomalies are to be used as data requires special consideration: a mean anomaly is defined over a "rectangular" block ( $\Delta\phi, \Delta\lambda$ ) ; consequently, the linear functionals which have to be applied to the covariance function involves an integration over that particular rectangle. Because of the structure of the kernel (covariance function), such integrations could be performed only approximately by a proper numerical integration method, a practically impossible enterprise: first, because of the tremendous computational effort, and second, because of the approximations involved. (Integrating the covariance function numerically over a certain region means approximating the covariance function by a set of locally restricted polynomials, usually step functions. Such covariance approximations introduce spectrum disturbances resulting in partly negative eigenvalues from a certain degree on (Sünkel, 1978). By numerical integration of the covariance function we, therefore, trade in an integrated effect in terms of possible singularities of the (anyway, not very stable) covariance matrix.) For these reasons, it is virtually inevitable to replace the covariances between mean values at zero altitude by expressions which avoid covariance integrations. Two considerations, which go back to C.C. Tscherning (Tscherning and Rapp, 1974, p. 70), lead to the replacement of a mean anomaly at zero altitude by a corresponding point anomaly at some specified altitude, depending on the block size and on the parameters of the covariance function : a) re-

placing the rectangular blocks over which the mean anomalies are defined by circular regions of equal size, it can be shown that the corresponding mean anomaly covariance function is obtained through a multiplication of the degree variances by the square of the eigenvalues of the moving average operator (Schwarz, 1976, p. 35 ff.). The corresponding infinite series, however, can no longer be represented by a closed covariance expression; the infinite series, could, for practical purposes, be terminated at a certain degree  $n \approx 200$  for  $5^\circ \times 5^\circ$ ,  $n \approx 3000$  for  $5' \times 5'$  block size), the summations, however, are too time consuming. Therefore, there seems to be only one simple way to overcome this difficulty: b) replacing the squares of the eigenvalues of the moving average operator by the  $(n+1)$ 'th power of a quantity  $u < 1$ , with  $u$  optimally fitted.  $u^{n+1}$  can be easily combined with  $(R_B^2/r_p r_Q)^{n+1}$  which leads to two interpretations: either a diminishing of the radius of the Bjerhammar sphere  $R_B$  or an upward continuation of the covariance function to a certain altitude leaving  $R_B$  unchanged; personally I find the latter interpretation more logical; moreover, it preserves consistency in the domain of homonicity. The  $u$ -values and altitudes corresponding to different block sizes can be found in (Schwarz, 1976, p. 39).

Keeping these conceptual replacements in mind, we can from now on formally consider mean gravity anomalies in zero altitude as point gravity anomalies in a certain elevation. In the following, some practical and theoretical considerations are made which put emphasis on the structure of the covariance matrix for gridded data.

### 3.1 Collocation solution for gridded data

The following studies deal with regularly distributed mean anomalies, which, for reasons explained before, can be treated like gridded point values. The coverage is unfortunately not total (mean anomalies of constant block sizes are restricted to rectangular zones surrounding the computation point). A total coverage of the sphere with gridded homogeneous data could be treated in a very fast and elegant way taking advantage of all existing symmetries (Colombo, 1979). Even in the case of a partial gridded data coverage, however, the structure of the data distribution carries over to the structure of the corresponding covariance matrix. These structures can advantageously be exploited in setting up and inverting the covariance matrix.

Let us illustrate such a typical structure by means of a very simple example: a geographical grid of data with 4 rows (parallels) and 6 columns (meridians) (Fig. 3.1). Parallels are assumed to be equally spaced by  $\Delta\phi$  and meridians are assumed to be equally spaced by  $\Delta\lambda$ .

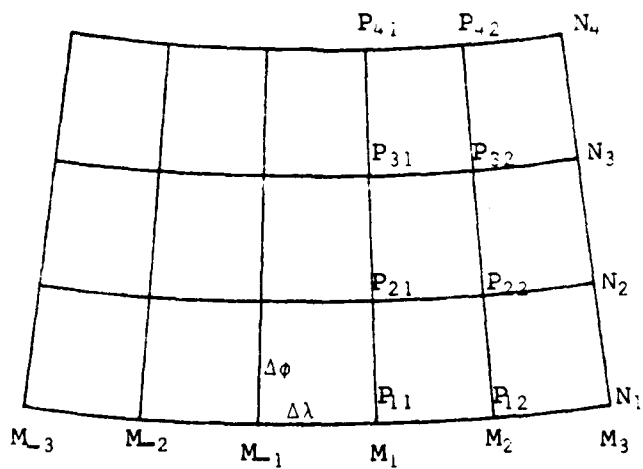


FIG. 3.1 Gridded data arrangement

The corresponding covariance matrix is a  $6 \cdot 4 \times 6 \cdot 4$  matrix. We partition the covariance matrix into  $6 \times 6$  submatrices each having dimension  $4 \times 4$  in accordance with the number of columns (6) and rows (4). The arrangement should be made such that the column counting is  $M_1, M_2, M_3, M_{-1}, M_{-2}, M_{-3}$  (from inside towards outside). If we denote the  $(4 \times 4)$  covariance matrix between two columns separated by  $m\Delta\lambda$  with  $C_m$ , the full covariance matrix has the following structure:

$$C = \begin{bmatrix} C_0 & C_1 & C_2 & | & C_1 & C_2 & C_3 \\ C_1 & C_0 & C_1 & | & C_2 & C_3 & C_4 \\ C_2 & C_1 & C_0 & | & C_3 & C_4 & C_5 \\ \hline C_1 & C_2 & C_3 & | & C_0 & C_1 & C_2 \\ C_2 & C_3 & C_4 & | & C_1 & C_0 & C_1 \\ C_3 & C_4 & C_5 & | & C_2 & C_1 & C_0 \end{bmatrix} \quad (3.3)$$

Three properties can be derived from (3.3) immediately:

- a)  $C$  has only 6 different submatrices  $C_0, \dots, C_5$ ,
- b)  $C$  can be partitioned into  $2 \times 2$  blocks

$$C = \begin{pmatrix} E & F \\ F & E \end{pmatrix} \quad (3.4a)$$

with

$$E = \begin{pmatrix} C_0 & C_1 & C_2 \\ C_1 & C_0 & C_1 \\ C_2 & C_1 & C_0 \end{pmatrix} \quad \text{and} \quad F = \begin{pmatrix} C_1 & C_2 & C_3 \\ C_2 & C_3 & C_4 \\ C_3 & C_4 & C_5 \end{pmatrix} . \quad (3.4b)$$

c) The row-sum of  $C$  equals  $E + F$  and is constant - a very important property which will be shown to account for substantial reductions in the inversion time.

The submatrix  $C_0$  (covariance matrix of column  $M_1$  with itself) is structured like  $E$ , the other submatrices  $C_i$ ,  $i > 0$  (covariance matrix of two distinct columns separated by  $i \cdot \Delta \lambda$ ) are structured like  $F$ ; e.g.

$$C_0 = \begin{bmatrix} C_{00}^0 & C_{01}^0 & C_{02}^0 & C_{03}^0 \\ C_{01}^0 & C_{00}^0 & C_{01}^0 & C_{02}^0 \\ C_{02}^0 & C_{01}^0 & C_{00}^0 & C_{01}^0 \\ C_{03}^0 & C_{02}^0 & C_{01}^0 & C_{00}^0 \end{bmatrix}; \quad C_1 = \begin{bmatrix} C_{00}^1 & C_{01}^1 & C_{02}^1 & C_{03}^1 \\ C_0^1 & C_{11}^1 & C_{12}^1 & C_{13}^1 \\ C_{02}^1 & C_{12}^1 & C_{22}^1 & C_{23}^1 \\ C_{03}^1 & C_{13}^1 & C_{23}^1 & C_{33}^1 \end{bmatrix}$$

(3.4c)

Consequently, we observe two levels of structurization: the column-structure ( $C_0, \dots, C_5$ ) and the block-structure ( $E, F$ ).

#### Quadratic matrices with constant row-sum

In connection with probability theory we will sometimes find matrices for which the sum of the row-elements is constant and equal to  $C$ . It can be shown (Zurmühl, 1964, p. 221 ff.) that the corresponding inverse has also a constant row-sum equal to  $1/C$ .

This fact leads to the question whether a generalization is possible such that the elements of the matrix are themselves submatrices.

Theorem: Let  $C$  be a non-singular quadratic matrix consisting of quadratic submatrices of equal size, and let the row-sum be constant and equal to  $\Sigma$ . Then  $C^{-1}$  consists of quadratic submatrices of equal size and has a constant row-sum equal to  $\Sigma^{-1}$ .

Proof: Obviously,  $C$  has an eigenvector-matrix  $S$  whose elements are unit-matrices, and  $\Sigma$  is the eigenvalue-matrix,

$$CS = S\Sigma \quad . \quad (3.5a)$$

It follows immediately that  $S$  is also the eigenvector-matrix of  $C^{-1}$ ; the eigenvalue-matrix is  $\Sigma^{-1}$ :

$$C^{-1}S = S\Sigma^{-1} \quad . \quad (3.5b)$$

Consequently,  $\Sigma^{-1}$  is the row-sum of the submatrices of  $C^{-1}$ .  $\square$

In our example this means that

$$C = \begin{pmatrix} E & F \\ F & E \end{pmatrix}, \quad \Sigma = E + F, \quad (3.6)$$

$$C^{-1} = \begin{pmatrix} G & H \\ H & G \end{pmatrix}, \quad G + H = (E + F)^{-1}.$$

What are the consequences for the estimation of the accuracy of a gravity field quantity like  $\delta_r$  at a point  $P$ , located on the line of symmetry with respect to the data grid?

Let us consider the cross-covariance vector  $C_p$ ; it relates (statistically) the predicted quantity at  $P$  with all the other

data. Since the data are regularly distributed on a grid, whose line of symmetry passes the prediction point  $P$ , it follows that  $C_p$  consists of two subvectors which are equal to each other,

$$C_p = \begin{pmatrix} C_{P1} \\ C_{P1} \end{pmatrix} ; \quad (3.7)$$

( $C_{P1}$  is the cross-covariance vector between the predicted quantity at  $P$  and all gridded data east of  $P$ ; it is at the same time the cross-covariance vector between the predicted quantity at  $P$  and all gridded data west of  $P$ .) Introducing (3.6) and (3.7) into the error estimation equation (3.1), we obtain

$$m_p^2 = C_{PP} - \left( C_{P1}^T, C_{P1}^T \right) \begin{pmatrix} G & H \\ H & G \end{pmatrix} \begin{pmatrix} C_{P1} \\ C_{P1} \end{pmatrix}$$

which obviously reduces to

$$m_p^2 = C_{PP} - 2 C_{P1}^T (G + H) C_{P1}$$

or

$m_p^2 = C_{PP} - 2 C_{P1}^T (E + F)^{-1} C_{P1} . \quad (3.8)$

(In the derivations above it was tacitly assumed that the data were free of noise; it can easily be shown, however, that (3.8) holds also if constant noise is introduced with error covariances dependent on the spherical distance.)

Equation (3.8) shows, how one single symmetry in the data pattern (here: symmetry with respect to the meridian of the pre-

diction point  $P$ ) can advantageously be used to reduce the computational effort drastically: apart from the substantial reduction in the number of covariance calculations, an application of the above theorem leads to splitting the size of the covariance matrix into a half. Since matrix inversion times increase with the 3rd power of its dimension, we conclude that a gain in speed of a factor 8 is rendered possible.

So far only symmetry with respect to the meridian has been considered. This is the case to be studied here (latitude of the prediction point is different from zero). The principle described above, however, can also be applied if two symmetries exist: symmetry with respect to the meridian and symmetry with respect to the equator. In order to take advantage of this special case, the prediction point  $P$  needs to coincide with the center of symmetry ( $\phi_p = 0$ ).

In Fig. 3.2 a data pattern of this kind is symbolically illustrated (each circle represents a grid of meridians and parallels).

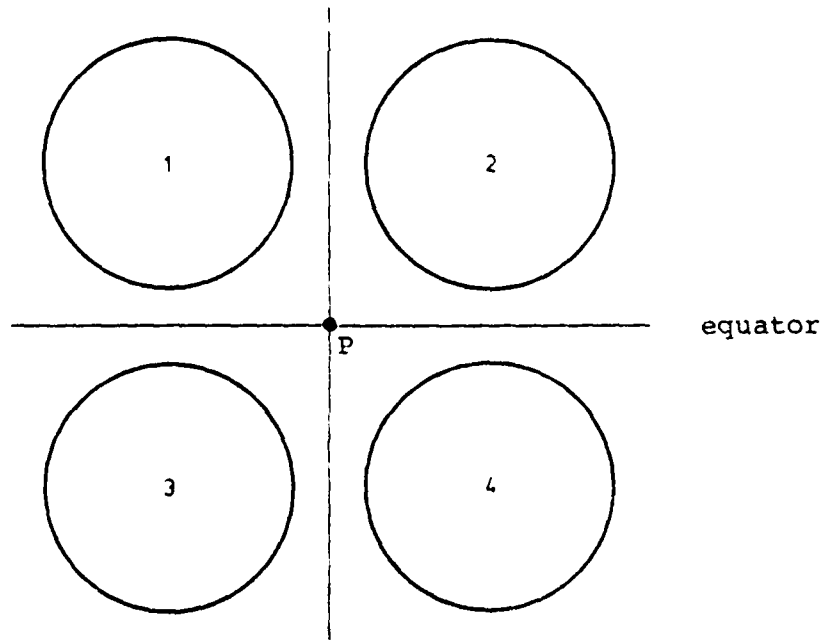


FIG. 3.2 Symmetry with respect to meridian and equator.

The covariance matrix consists of 4 submatrices (2 in the former case)

$$C = \begin{bmatrix} C_{11} & C_{12} & C_{13} & C_{14} \\ C_{12} & C_{11} & C_{14} & C_{13} \\ C_{13} & C_{14} & C_{11} & C_{12} \\ C_{14} & C_{13} & C_{12} & C_{11} \end{bmatrix} \quad (3.9)$$

The row-sum is obviously constant and equal to  $\Sigma$  with

$$\Sigma = C_{11} + C_{12} + C_{13} + C_{14} . \quad (3.10)$$

In analogy to (3.7) the cross-covariance vector between the predicted quantity at  $P$  and the data consists of 4 equal subvectors,

$$C_P = \begin{bmatrix} C_{P1} \\ C_{P1} \\ C_{P1} \\ C_{P1} \end{bmatrix} . \quad (3.11)$$

Observing the above theorem, the error estimation equation (3.1) can be expressed by

$$m_p^2 = C_{PP} - \left( C_{P1}^T, C_{P1}^T, C_{P1}^T, C_{P1}^T \right) \begin{bmatrix} K_{11} & K_{12} & K_{13} & K_{14} \\ K_{12} & K_{11} & K_{14} & K_{13} \\ K_{13} & K_{14} & K_{11} & K_{12} \\ K_{14} & K_{13} & K_{12} & K_{11} \end{bmatrix} \begin{bmatrix} C_{P1} \\ C_{P1} \\ C_{P1} \\ C_{P1} \end{bmatrix} \quad (3.12a)$$

with

$$K_{11} + K_{12} + K_{13} + K_{14} = \Sigma^{-1} . \quad (3.12b)$$

Consequently, the mean square error is simply given by

$$m_p^2 = C_{pp} - 4 C_{p1}^T (C_{11} + C_{12} + C_{13} + C_{14})^{-1} C_{p1} . \quad (3.13)$$

It should again be noted that this error estimation equation is valid if the data pattern has two lines of symmetry with respect to the prediction point. The size of the original covariance matrix to be inverted is split into 4 ; therefore, a gain in speed by a factor of 64 can be expected in this case of meridional and equatorial symmetry.

## 4. INTEGRAL APPROACH

It is well-known that the disturbing potential  $T$  can be expressed in terms of free air anomalies  $\Delta g$  by

$$T(r, \phi, \lambda) = \frac{R}{4\pi} \iint_{\sigma} S(r, \psi) \Delta g d\sigma \quad (4.1a)$$

with  $S(r, \psi)$  denoting the spatial Stokes kernel

$$S(r, \psi) = \frac{2R}{l} + \frac{R}{r} - 3 \frac{Rl}{r^2} - \frac{R^2}{r^2} \cos\psi \left[ 5 + 3 \ln \frac{r-R\cos\psi+1}{2r} \right] \quad (4.1b)$$

(Heiskanen and Moritz, 1967, p. 233).

$R$  stands for the mean radius of the earth,  $\psi$  for the spherical distance and  $l$  for the spatial distance between two points,

$$l = (r^2 + R^2 - 2rR\cos\psi)^{1/2} \quad (4.1c)$$

The quantity of interest is the gradient of  $T$

$$\text{grad } T = \frac{R}{4\pi} \iint_{\sigma} \text{grad}_P S(P, Q) \Delta g(Q) d\sigma(Q) ,$$

represented in terms of 3 components

$$\begin{aligned} \delta_r(P) &= \frac{R}{4\pi} \iint_{\sigma} D_r P S(P, Q) \Delta g(Q) d\sigma(Q) , \\ \delta_\phi(P) &= \frac{R}{4\pi r} \iint_{\sigma} D_\phi P S(P, Q) \Delta g(Q) d\sigma(Q) , \end{aligned} \quad (4.2)$$

$$\delta_\lambda(P) = \frac{R}{4\pi r_p \cos \phi_p} \iint_{\sigma} D_\lambda S(P, Q) \Delta g(Q) d\sigma(Q) . \quad (4.2)$$

If the gravity anomalies would be known at all points of  $\sigma$  and, in addition,  $\Delta g$  would be free of noise, grad T could be predicted at any point P outside the surface of the earth introducing errors only due to spherical approximation and due to minor conceptual neglections in the definition of  $\Delta g$ ; a detailed discussion can be found in (Heiskanen and Moritz, 1967, p. 240 ff.).

Naturally, the above two conditions are never fulfilled: the function  $\Delta g$ , postulated by (4.2), is usually available in terms of a step-function approximation (= mean gravity anomalies defined on rectangular blocks); in addition, these mean anomalies are never error-free. Therefore, two additional errors are introduced in the calculation of grad T : a representation error (step function representation of the true function  $\Delta g$ ), and a data error (upward continued integrated effect of data-noise). The following two sections deal with the estimation of both errors.

#### 4.1 Estimation of the representation error

As mentioned before, the (unknown) actual function  $\Delta g$  is approximated by a step function; the size of the steps equal the varying size of the blocks (cf. Table 2.1). Representing a function (different from a constant) by its mean values means loss of information, particularly in the higher frequencies. The goal is to estimate the average effect of such information deficiencies onto the gradient of the disturbing potential in high altitudes. Such

an estimation requires, for practical reasons, two assumptions:

- a) replacement of the step function defined over rectangular blocks by a moving average of the function, such that the averaging region is a circle with an area equal to the block area;
- b) replacement of the rectangular zones in which the mean values are given (cf. Fig. 2.1) by circular zones of equal size.

These simplifications are introduced in order to obtain isotropic operators; note that similar assumptions have been made for the ~~collocation~~ solution.

#### Eigenvalues of integral operators with isotropic kernel

Integral operators with isotropic kernel play a fundamental role in representation error estimation procedures. Therefore, a brief sketch of basic relations will be given in the sequel; it is essentially an outline of (Meissl, 1971b, p. 38ff.).

Consider the integral transformation

$$g(P) = \iint_{\sigma} K(P, Q) f(Q) d\sigma(Q) \quad (4.3a)$$

with an isotropic kernel  $K$ ,

$$K(P, Q) = K(\cos\psi) . \quad (4.3b)$$

According to the Funck-Hecke formula (Müller, 1966, p.20), the spherical harmonics  $\{\phi_{nm}\}$  are eigenfunctions of this integral transformation; the eigenvalues  $\kappa_n$  are projections of the kernel onto the Legendre polynomials,

$$\iint_{\sigma} K(P, Q) \phi_{nm}(Q) d\sigma(Q) = \kappa_n \phi_{nm}(P) \quad (4.4a)$$

with

$$\kappa_n = 2\pi \int_{-1}^1 K(t) P_n(t) dt . \quad (4.4b)$$

An isotropic integral kernel can be represented in terms of a series of Legendre polynomials,

$$K(t) = \sum_n k_n P_n(t) ; \quad (4.5a)$$

applying (4.4b) and the orthogonality relation of Legendre polynomials,

$$\int_{-1}^1 P_n(t) P_m(t) = \frac{2}{2n+1} \delta_{nm} ,$$

it follows that the eigenvalues of  $K$  are given by

$$\kappa_n = \frac{4\pi}{2n+1} k_n . \quad (4.5b)$$

Let

$$f(P) = \sum_{n,m} f_{nm} \phi_{nm}(P) \quad \text{and} \quad g(P) = \sum_{n,m} g_{nm} \phi_{nm}(P)$$

be spherical harmonic expansions of  $f$  and  $g$ , respectively; then

$$g_{nm} = \kappa_n f_{nm} \quad (4.6)$$

follows from (4.4a,b). Equation (4.6) is the frequency domain analogue of the integral transformation (4.3a). It will play a central role in the following.

The moving average operator

If the isotropic kernel  $B(t)$  of an integral transformation like (4.3a) is constant for  $t \geq t_0 > -1$  and vanishes outside,  $B$  is called a moving average kernel,

$$B(t) = \begin{cases} \frac{1}{2\pi(1-t_0)} & \text{for } t_0 \leq t \leq 1 \\ 0 & \text{else} \end{cases} . \quad (4.7)$$

Its eigenvalues  $\beta_n$  are obtained by an application of equation (4.4b); as a matter of fact, they depend on  $t_0$ ,

$$\beta_n(t_0) = \frac{1}{1-t_0} \int_{t_0}^1 P_n(t) dt .$$

The following expression can be found in (Meissl, 1971a, p. 24) :

$$\beta_n(t_0) = \frac{1}{1-t_0} \frac{1}{2n+1} [P_{n-1}(t_0) - P_{n+1}(t_0)] . \quad (4.8)$$

It follows from a Taylor-linearization of  $P_n(t)$  at  $t = 1$  that

$$\beta_n(1) \equiv 1 \quad (\dots \text{function reproduction}) . \quad (4.8)'$$

Due to the orthogonality of Legendre polynomials we obtain

$$\beta_n(-1) = \delta_{n0} (\dots \text{function annihilation}) .$$

Any other moving average operator will function between these two extreme cases, reproduction and annihilation.

It is now a simple task to find the loss of information introduced by applying a moving average operator onto a function  $f$ ,

$$\delta f(P) := f(P) - \bar{f}(P) = \sum_{n,m} [1 - \beta_n(t_0)] f_{nm} \phi_{nm}(P) . \quad (4.9)$$

### The spatial Stokes kernel and its radial derivative

The disturbing potential can be represented by a series of solid spherical harmonics

$$T(r, \theta, \lambda) = \sum_{n=2}^{\infty} \left(\frac{R}{r}\right)^{n+1} T_n(\theta, \lambda) ; \quad (4.10)$$

taking into account the relation between the disturbing potential  $T$  and the gravity anomaly  $\Delta g$  in the frequency domain

$$T_{nm} = \frac{R}{n-1} \Delta g_{nm} , \quad (4.11)$$

$T$  can be formulated in terms of  $\Delta g$ ,

$$T(r, \theta, \lambda) = R \sum_{n=2}^{\infty} \left(\frac{R}{r}\right)^{n+1} \frac{1}{n-1} \Delta g_n(\theta, \lambda) ,$$

which, by expressing the Laplace spherical harmonic  $\Delta g_n(\theta, \lambda)$  explicitly, goes over into

$$T(r, \theta, \lambda) = \frac{R}{4\pi} \iint \left[ \sum_{n=2}^{\infty} \left(\frac{R}{r}\right)^{n+1} \frac{2n+1}{n-1} P_n(\cos\psi) \right] \Delta g d\sigma .$$

The infinite sum is known as the spatial Stokes function  $S(r, \psi)$  which is given in its closed form by equation (4.1b),

$$S(r, \psi) = \sum_{n=2}^{\infty} \left(\frac{R}{r}\right)^{n+1} \frac{2n+1}{n-1} P_n(\cos\psi) . \quad (4.12)$$

It is the upward continued Stokes kernel  $S(R, \psi)$ . Its radial derivative follows immediately,

$$D_r S(r, \psi) = - \frac{1}{r} \sum_{n=2}^{\infty} \left(\frac{R}{r}\right)^{n+1} \frac{(2n+1)(n+1)}{n-1} P_n(\cos\psi) . \quad (4.13)$$

Eigenvalues of the kernel  $- \frac{r}{2\pi} D_r S(r, \psi)$  truncated at  $\psi = \psi_n$

In order to estimate the impact of neglecting  $\Delta g$  - information in circular zones around the computation point on  $\delta_r$ , it is essential to know the eigenvalue of the corresponding truncated kernel.

If the kernel  $-r/2\pi D_r S(r, \psi)$  vanishes for  $\psi < \psi_0$ , its eigenvalues are obtained by applying equation (4.4b) ,

$$s'_n(r, t_0) = \sum_{k=2}^{\infty} \left( \frac{R}{r} \right)^{k+1} \frac{(2k+1)(k+1)}{k-1} \int_{-1}^{t_0} P_n(t) P_k(t) dt. \quad (4.14)$$

According to (Paul, 1973), the integral of products of Legendre functions is given by

$$\begin{aligned} R_{nk} &:= \int_{-1}^{t_0} P_n(t) P_k(t) dt \\ &= \frac{1}{(n-k)(n+k+1)} \left[ \frac{n(n+1)}{2n+1} P_k(P_{n+1} - P_{n-1}) - \frac{k(k+1)}{2k+1} (P_{k+1} - P_{k-1}) \right] \end{aligned} \quad (4.15a)$$

for  $n \neq k$  , and the recursion formula

$$R_{nn} = \frac{(n+1)(2n-1)}{n(2n+1)} R_{n+1, n-1} - \frac{n-1}{n} R_{n, n-2} + \frac{2n-1}{2n+1} R_{n-1, n-1}$$

$$(4.15b)$$

for  $n = k$  ; (here and in the sequel we suppress the argument  $t_0$ )

for the sake of simplicity.) Initial values are

$$\begin{aligned} R_{00} &= 1 + t_0 \\ R_{11} &= (1 + t_0^3)/3 . \end{aligned} \quad (4.15c)$$

What follows, is a tour de force, the attempt to find a closed expression for the infinite sum in equation (4.14).

Denoting  $R/r$  by  $\rho$  and using the relations (4.15a,b), the eigenvalues  $s'_n$  are given by

$$s'_n(r, t_0) = \sum_{\substack{k=2 \\ k \neq n}}^{\infty} \frac{(2k+1)(k+1)}{k-1} \rho^{k+1} R_{nk} + \frac{(2n+1)(n+1)}{n-1} \rho^{n+1} R_{nn} . \quad (4.16a)$$

Explicitly written

$$\begin{aligned} s'_n &= \frac{n(n+1)}{2n+1} (P_{n+1} - P_{n-1}) \sum_{\substack{k=2 \\ n \neq k}}^{\infty} \frac{(2k+1)(k+1)}{(k-1)(n-k)(n+k+1)} \rho^{k+1} P_k \\ &\quad + \rho P_n \sum_{\substack{k=1 \\ k \neq n-1}}^{\infty} \frac{(k+2)^2(k+1)}{k(n-k-1)(n+k+2)} \rho^{k+1} P_k \\ &\quad - \frac{1}{\rho} P_n \sum_{\substack{k=3 \\ k \neq n+1}}^{\infty} \frac{k^2(k-1)}{(k-2)(n-k+1)(n+k)} \rho^{k+1} P_k + \frac{(2n+1)(n+1)}{n-1} \rho^{n+1} R_{nn} . \end{aligned} \quad (4.16b)$$

We know (Tscherning, 1972) that closed expressions are available for series of the following general form:

$$F_\alpha(\rho, t) := \sum_{k=0}^{\infty} \frac{1}{k+\alpha} \rho^{k+1} P_k(t), \quad \alpha > 0 \quad (4.17a)$$

and

$$F_\alpha(\rho, t) = \sum_{k=1-\alpha}^{\infty} \frac{1}{k+\alpha} \rho^{k+1} P_k(t), \quad \alpha \leq 0 \quad (4.17b)$$

(Moritz, 1980, p. 186) where  $\alpha$  denotes a fixed integer. Therefore, we express the coefficients of the Legendre functions in terms of partial fractions of the form  $(k \pm \alpha)^{-1}$ ; the following identities can immediately be verified :

$$\begin{aligned} \frac{(2k+1)(k+1)}{(k-1)(n-k)(n+k+1)} &= \frac{6}{(n+2)(n-1)} \frac{1}{k-1} - \frac{n+1}{n-1} \frac{1}{k-n} \\ &\quad - \frac{n}{n+2} \frac{1}{k+n+1}, \end{aligned} \quad (4.18a)$$

$$\begin{aligned} \frac{(k+2)^2(k+1)}{k(n-k-1)(n+k+2)} &= \frac{4}{(n+2)(n-1)} \frac{1}{k} - \frac{n(n+1)^2}{(2n+1)(n-1)} \frac{1}{k-(n-1)} \\ &\quad + \frac{n^2(n+1)}{(2n+1)(n+2)} \frac{1}{k+n+2} - 1, \end{aligned} \quad (4.18b)$$

$$\begin{aligned} \frac{k^2(k-1)}{(k-1)(n-k+1)(n+k)} &= \frac{4}{(n+2)(n-1)} \frac{1}{k-2} - \frac{n(n+1)^2}{(2n+1)(n-1)} \frac{1}{k-(n+1)} \\ &\quad + \frac{n^2(n+1)}{(2n+1)(n+2)} \frac{1}{k+n} - 1. \end{aligned} \quad (4.18c)$$

Introducing these partial fractions into (4.16b) leads to infinite sums of the following kind:

	A	B	C
1	$\sum_{k=2}^{\infty} \frac{1}{k-1} \rho^{k+1} p_k$ $k \neq n$	$\sum_{k=1}^{\infty} \frac{1}{k} \rho^{k+1} p_k$ $k \neq n-1$	$\sum_{k=3}^{\infty} \frac{1}{k-2} \rho^{k+1} p_k$ $k \neq n+1$
2	$\sum_{k=2}^{\infty} \frac{1}{k-n} \rho^{k+1} p_k$ $k \neq n$	$\sum_{k=1}^{\infty} \frac{1}{k-(n-1)} \rho^{k+1} p_k$ $k \neq n-1$	$\sum_{k=3}^{\infty} \frac{1}{k-(n+1)} \rho^{k+1} p_k$ $k \neq n+1$
3	$\sum_{k=2}^{\infty} \frac{1}{k+n+1} \rho^{k+1} p_k$ $k \neq n$	$\sum_{k=1}^{\infty} \frac{1}{k+n+2} \rho^{k+1} p_k$ $k \neq n-1$	$\sum_{k=3}^{\infty} \frac{1}{k+n} \rho^{k+1} p_k$ $k \neq n+1$
4		$\sum_{k=1}^{\infty} \rho^{k+1} p_k$ $k \neq n-1$	$\sum_{k=3}^{\infty} \rho^{k+1} p_k$ $k \neq n+1$

TABLE 4.1 Infinite series with closed expressions.

Using the notation of (4.17a,b), closed expressions are available for  $\alpha \geq -2$  in (Moritz, 1980, p. 187, 188); only the elements of the 2nd row in Table 4.1 pose problems:

Paul (1973, p. 418 ff.) defines a quantity

$$U_n(t, \rho) := \sum_{\substack{k=0 \\ k \neq n-1}}^{\infty} \frac{1}{k-(n-1)} \rho^{k-(n-1)} P_k(t) \quad (4.19)$$

and arrives, after very elegant operations, at the relation

$$\begin{aligned} (n-1)U_n(t, \rho) &= (2n-3)tU_{n-1}(t, \rho) + (n-2)U_{n-2}(t, \rho) \\ &+ \frac{L}{\rho^{n-1}} = (n-1)U_n(t, 1) - (2n-3)tU_{n-1}(t, 1) \\ &+ (n-2)U_{n-2}(t, 1) + \sqrt{2-2t} \end{aligned} \quad (4.20)$$

with the auxiliary quantity

$$L := \sqrt{1-2\rho t+\rho^2} ; \quad (4.21)$$

After some manipulations, he derives a recurrence relation for  $U_n(t, 1)$ ,

$$U_n(t, 1) = \frac{1}{n-1} \left[ (2n-3)tU_{n-1}(t, 1) - (n-2)U_{n-2}(t, 1) \right. \\ \left. - \sqrt{2-2t} + \frac{P_{n-3}(t) - P_{n-1}(t)}{2n-3} \right] . \quad (4.22)$$

Equation (4.20) and (4.22) enable us to derive a general recurrence relation for  $U_n(t, \rho)$

$$U_n(t, \rho) = \frac{1}{n-1} \left[ (2n-3)tU_{n-1}(t, \rho) - (n-2)U_{n-2}(t, \rho) \right. \\ \left. - \frac{L}{\rho^{n-1}} + \frac{P_{n-3}(t) - P_{n-1}(t)}{2n-3} \right] . \quad (4.23)$$

$U_n(t, \rho)$  can also be related to  $F_\alpha$  defined in (4.17); recalling the definition (4.19), we obtain

$$F_{-n} = \rho^{n+1} U_{n+1} - \sum_{k=0}^{n-1} \frac{1}{k-n} \rho^{k+1} p_k$$

and after straightforward operations involving the substitution of (4.23), we finally find a recurrence relation for  $F_{-n}$ ,

$$\begin{aligned} F_{-n} &= \frac{2n-1}{n} t\rho \left( \sum_{k=0}^{n-2} \frac{1}{k-(n-1)} \rho^{k+1} p_k + F_{-(n-1)} \right) \\ &\quad - \frac{n-1}{n} \rho^2 \left( \sum_{k=0}^{n-3} \frac{1}{k-(n-2)} \rho^{k+1} p_k + F_{-(n-2)} \right) \\ &\quad - \rho \left( \sum_{k=0}^{n-1} \frac{1}{k-n} \rho^{k+1} p_k + \frac{L}{n} \right) + \rho^{n+1} \frac{p_{n-2} - p_n}{n(2n-1)} . \end{aligned} \quad (4.24)$$

With the initial values

$$U_0(t, \rho) = F_1(t, \rho) = \ln \left( 1 + \frac{2\rho}{1-\rho+L} \right) ,$$

$$U_1(t, \rho) = \frac{1}{\rho} F_0(t, \rho) = \ln \left( \frac{2}{N} \right) ,$$

$$(N := 1 + L - \rho t) ,$$

we find  $U_n$  for arbitrary  $n$  by applying the recursion formula (4.23).

$F_n$  with  $n > 0$  and a corresponding recurrence relation can be found in (Moritz, 1980, p. 188) :

$$F_1(t, \rho) = U_0(t, \rho) ,$$

$$F_2(t, \rho) = \frac{1}{\rho} [L - 1 + tF_1(t, \rho)] , \quad (4.25)$$

$$F_{n+1}(t, \rho) = \frac{1}{n\rho} [L + (2n-1)tF_n(t, \rho) - \frac{(n-1)}{\rho} F_{n-1}(t, \rho)] .$$

These are the cumbersome prerequisites which enable us to express all infinite series of Table 4.1 in a closed form:

$$A1 : \sum_{\substack{k=2 \\ k \neq n}}^{\infty} \frac{1}{k-1} \rho^{k+1} p_k = F_{-1} - \frac{1}{n-1} \rho^{n+1} p_n ,$$

$$A2 : \sum_{\substack{k=2 \\ k \neq n}}^{\infty} \frac{1}{k-n} \rho^{k+1} p_k = \rho^{n+1} U_{n+1} + \rho \left( \frac{1}{n} + \frac{\rho t}{n-1} \right) , \quad (4.26a)$$

$$A3 : \sum_{\substack{k=2 \\ k \neq n}}^{\infty} \frac{1}{k+n+1} \rho^{k+1} p_k = F_{n+1} - \frac{\rho}{n+1} - \frac{\rho^2}{n+2} p_1 - \frac{\rho^{n+1}}{2n+1} p_n ,$$

$$B1 : \sum_{\substack{k=1 \\ k \neq n-1}}^{\infty} \frac{1}{k} \rho^{k+1} p_k = F_0 - \frac{1}{n-1} \rho^n p_{n-1} ,$$

(4.26b)

$$B2 : \sum_{\substack{k=1 \\ k \neq n-1}}^{\infty} \frac{1}{k-(n-1)} \rho^{k+1} p_k = \rho^n U_n + \frac{\rho}{n-1} ,$$

$$B3 : \sum_{\substack{k=1 \\ k \neq n-1}}^{\infty} \frac{1}{k+n+2} \rho^{k+1} p_k = F_{n+2} - \frac{\rho}{n+2} - \frac{\rho^n}{2n+1} p_{n-1},$$

(4.26b)

$$B4 : \sum_{\substack{k=1 \\ k \neq n-1}}^{\infty} \rho^{k+1} p_k = \rho \left( \frac{1}{L} - 1 \right) - \rho^n p_{n-1},$$

$$C1 : \sum_{\substack{k=3 \\ k \neq n+1}}^{\infty} \frac{1}{k-2} \rho^{k+1} p_k = F_{-2} - \frac{1}{n-1} \rho^{n+2} p_{n+1},$$

$$C2 : \sum_{\substack{k=3 \\ k \neq n+1}}^{\infty} \frac{1}{k-(n+1)} \rho^{k+1} p_k = \rho^{n+2} U_{n+2} + \rho \left( \frac{1}{n+1} + \frac{\rho P_1}{n} + \frac{\rho^2 P_2}{n-1} \right),$$

$$C3 : \sum_{\substack{k=3 \\ k \neq n+1}}^{\infty} \frac{1}{k+n} \rho^{k+1} p_k = F_n - \rho \left( \frac{1}{n} + \frac{\rho}{n+1} P_1 - \frac{\rho^2}{n+2} P_2 - \frac{\rho^{n+1}}{2n+1} P_{n+1} \right),$$

$$C4 : \sum_{\substack{k=3 \\ k \neq n+1}}^{\infty} \rho^{k+1} p_k = \rho \left( \frac{1}{L} - 1 - \rho P_1 - \rho^2 P_2 - \rho^{n+1} P_{n+1} \right).$$

(4.26c)

With (4.18) and (4.26)  $s'_n$  can be expressed by

$$\begin{aligned}
 s_n' &= \frac{n(n+1)}{(2n+1)} (P_{n+1} - P_{n-1}) \left[ \frac{6}{(n+2)(n-1)} A_1 - \frac{n+1}{n-1} A_2 - \frac{n}{n+2} A_3 \right. \\
 &\quad + \rho P_n \left[ \frac{4}{(n+2)(n-1)} B_1 - \frac{n(n+1)^2}{(2n+1)(n-1)} B_2 + \frac{n^2(n+1)}{(2n+1)(n+2)} B_3 - B_4 \right. \\
 &\quad - \frac{1}{\rho} P_n \left[ \frac{4}{(n+2)(n-1)} C_1 - \frac{n(n+1)^2}{(2n+1)(n-1)} C_2 + \frac{n^2(n+1)}{(2n+1)(n+2)} C_3 - \right. \\
 &\quad \left. \left. - C_4 \right] + \frac{(2n+1)(n+1)}{n-1} \rho^{n+1} R_{nn} \right];
 \end{aligned}
 \tag{4.27}$$

substituting  $A_i$ ,  $B_i$ , and  $C_i$ , the eigenvalues of the truncated kernel, defined in (4.16a), are finally given by

$$\begin{aligned}
s_n' &= \frac{n(n+1)}{2n+1} \left( P_{n+1} - P_{n-1} \right) \left[ \frac{6}{(n+2)(n-1)} \left( F_{-1} - \frac{1}{n-1} \rho^{n+1} P_n \right) \right. \\
&\quad - \frac{n+1}{n-1} \left( \rho^{n+1} U_{n+1} + \frac{\rho}{n} + \frac{\rho^2 P_1}{n-1} \right) - \frac{n}{n+2} \left( F_{n+1} - \frac{\rho}{n+1} - \frac{\rho^2 P_1}{n+2} \right. \\
&\quad \left. \left. - \frac{\rho^{n+1} P_n}{2n+1} \right) \right] \\
&\quad + P_n \left\{ \frac{4}{(n+2)(n-1)} \left[ \rho F_0 - \frac{1}{\rho} F_{-2} + \frac{\rho^{n+1}}{n-1} \left( P_{n+1} - P_{n-1} \right) \right] \right. \\
&\quad + \frac{n(n+1)^2}{(2n+1)(n-1)} \left[ \rho^{n+1} (U_{n+2} - U_n) + \frac{\rho^2}{n-1} (P_2 - P_0) + \frac{1}{n+1} + \frac{\rho P_1}{n} \right] \\
&\quad + \frac{n^2(n+1)}{(2n+1)(n+2)} \left[ \rho F_{n+2} - \frac{1}{\rho} F_n + \frac{\rho^2}{n+2} (P_2 - P_0) + \frac{\rho^{n+1}}{2n+1} \cdot \right. \\
&\quad \cdot \left. \left( P_{n+1} - P_{n-1} \right) + \frac{1}{n} + \frac{\rho}{n+1} P_1 \right] + (1 - \rho^2) \left( \frac{1}{L} - 1 \right) - \\
&\quad \left. - \rho^{n+1} \left( P_{n+1} - P_{n-1} \right) - \rho P_1 - \rho^2 P_2 \right\} + \frac{(2n+1)(n+1)}{n-1} \rho^{n+1} R_{nn} .
\end{aligned}$$

Again the dependence of  $t_0$  has been suppressed in  $P$ ,  $U$ ,  $F$ ,  $R$ , and  $s$ .

The eigenvalues  $s'_n$  have to fulfil various conditions; this enables us to roughly check the equation:

a)  $s'_n(\rho, -1) \equiv 0$  because of coinciding limits of integration;

b)  $s'_n(\rho, 1) = 2 \left( \frac{R}{r} \right)^{n+1} \frac{n+1}{n-1}$  for  $n \geq 2$ ; this follows from the orthogonality of the Legendre polynomials;

The interested reader will note the relation of  $s'_n$  to the so-called Molodensky coefficients  $Q_n$ , defined as the eigenvalues of the isotropic kernel  $S(\psi)/2\pi$ , where  $S(\psi)$  denotes Stokes' function (Heiskanen and Moritz, 1967, p. 259 ff.),

$$Q_n(t_0) := \int_{-1}^{t_0} S(t) P_n(t) dt ;$$

for  $t_0 = 1$  we obtain,

$$Q_n(1) = \frac{2}{n-1} ;$$

therefore  $s'_n(\rho, 1)$  is related to  $Q_n(1)$  by

$$\begin{aligned} s'_n(\rho, 1) &= \left( \frac{R}{r} \right)^{n+1} (n+1) Q_n \\ &= \left( \frac{R}{r} \right)^{n+1} 2(1+Q_n) . \end{aligned} \quad (4.29)$$

Formula (4.28) can easily be programmed; a very efficient routine has been developed which calculates 1000 coefficients for arbitrary

$\rho \leq 1$  and  $-1 \leq t_0 \leq 1$  within 0.9 seconds CPU-time on a Univac 1100. (This value agrees with an estimate obtained by Paul (1973, p. 422) for the computation of the Molodensky coefficients using an analogous procedure.)

Now we come back to the estimation of the representation error. Let the free air gravity anomaly  $f$  be expanded into a series of orthogonal spherical harmonics,

$$f(P_0) = \sum_{n,m} f_{nm} \phi_{nm}(P_0) ;$$

then we know from (4.6) that the gravity disturbance series expansion can simply be obtained through a multiplication of the coefficients by the eigenvalue which relates both quantities, the gravity disturbance at a fixed altitude and the gravity anomaly; denoting the gravity disturbance by  $\delta_r$ , it follows with (4.2) and (4.13) that

$$\delta_r(P) = -\frac{R}{2r} \sum_{n,m} s_n'(\rho, 1) f_{nm} \phi_{nm}(P)$$

is its spherical harmonic expansion expressed at the altitude of  $P$  in terms of gravity anomaly coefficients  $\{f_{nm}\}$ . If we neglect gravity information outside  $\psi = \psi_0$  around the computation point  $P$ , an error in  $\delta_r(P)$  is introduced which can simply be obtained by replacing the eigenvalue  $s_n'(\rho, 1)$  by the eigenvalue of the corresponding truncated kernel  $s_n'(\rho, t_0)$ ,

$$e_{\delta_r}(P) = -\frac{\rho}{2} \sum_{n,m} s_n'(\rho, t_0) f_{nm} \phi_{nm}(P) .$$

If in the same region the actual gravity anomaly function is replaced by its moving average, the coefficients are to be replaced by the

eigenvalue difference of the corresponding moving average operator

$$e_{\delta_r}(P) = -\frac{\rho}{2} \sum_{n,m} s'_n(\rho, t_0) [1 - \beta_n(\tau_0)] f_{nm} \phi_{nm}(P).$$

The principle should be clear: each integral transformation can be considered as a two-dimensional convolution on the sphere; it is well-known that a convolution of two functions in the space domain is equivalent to a multiplication of the corresponding spectral values in the frequency domain; in the case discussed above, two convolutions are performed successively.

In the case to be studied in this report, 5 regions are defined with various moving averages. Denoting the cosine of the radius of the moving average circle for region  $i$  by  $\tau_i$  and the cosine of the outer radius of the circular zone, in which this moving average is applied, by  $t_i$ , the representation error is obtained by adding the corresponding eigenvalue products,

$$e_{\delta_r}(P) = -\frac{\rho}{2} \sum_{n,m} \sum_{i=1}^I s'_n(\rho, t_{i-1}) [\beta(\tau_{i-1}) - \beta(\tau_i)] f_{nm} \phi_{nm}(P)$$
(4.30)

with

$$\beta_n(\tau_0) = \beta_n(1) \equiv 1 \quad \text{and} \quad t_0 = 1 ;$$

$I$  stands for the number of regions. With

$$\lambda'_n := \frac{\rho}{2} \sum_{i=1}^I s'_n(\rho, t_{i-1}) [\beta(\tau_{i-1}) - \beta(\tau_i)]$$
(4.31)

we can estimate the mean square representation error,

$$m_{\delta_r}^2 = M \left\{ e_{\delta_r}^2 (P) \right\} = M \left\{ \sum_{n,m} \lambda_n^2 f_{nm} \phi_{nm}(P) \sum_{r,s} \lambda_r^2 f_{rs} \phi_{rs}(P) \right\}$$

which, due to the orthogonality of the basis  $\{\phi_{nm}\}$ , reduces to

$$m_{\delta_r}^2 = \sum_{n,m} \lambda_n^2 f_{nm}^2 . \quad (4.32)$$

Recall that  $f_{nm}$  are the harmonic coefficients of the gravity anomaly's expansion into a series of fully normalized spherical harmonics. Therefore, the sum of  $f_{nm}^2$  taken over  $m$  represents the actual gravity anomaly degree variance  $c_n$  of degree  $n$ , (Heiskanen and Moritz, 1967, p. 259),

$$c_n := \sum_m f_{nm}^2 . \quad (4.33)$$

Empirical degree variances are available up to relatively small  $n$  (say  $n = 36$ ) ; higher degree variances have to be taken from a degree variance model like

$$c_n = A c_0^{n+2} \frac{n-1}{(n-1)(n+B)} , \quad n > 2 \quad (4.34)$$

with, e.g.

$$\begin{aligned} A &= 425 \text{ mgal}^2 , \\ c_0 &= 0.999617 , \\ B &= 24 , \\ c_2 &= 7.5 \text{ mgal}^2 \end{aligned}$$

(Tscherning, 1976). With (4.33) the mean square representation error is expressed by

$$\boxed{m_{\delta_r}^2 = \sum_{n=2}^{\infty} \lambda_n^2 c_n} \quad (4.35)$$

The eigenvalues  $s_n(\rho, t_0)$  of the truncated spatial Stokes kernel will be needed in order to derive the representation error's impact on the horizontal components of the gradient of the disturbing potential. With (4.4b) the eigenvalues of the kernel  $S(r, \psi)/2\pi$  are given by

$$s_n(\rho, t_0) = \int_{-1}^{t_0} S(r, t) P_n(t) dt,$$

which, by substituting equation (4.12) for  $S(r, t)$ , is expressed by

$$s_n(\rho, t_0) = \sum_{k=2}^{\infty} \frac{2k+1}{k-1} \left(\frac{R}{r}\right)^{k+1} \int_{-1}^{t_0} P_n(t) P_k(t) dt. \quad (4.36)$$

The integral is denoted  $R_{nk}$  as before; it can be expressed in closed form in terms of Legendre polynomials (equation (4.15a) for  $n \neq k$ , and (4.15b) for  $n = k$ ). With this notation the infinite series

$$s_n(\rho, t_0) = \sum_{\substack{k=2 \\ k \neq n}}^{\infty} \frac{2k+1}{k-1} \rho^{k+1} R_{nk} + \frac{2n+1}{n-1} \rho^{n+1} R_{nn}$$

has to be expressed in a closed form. Introducing (4.15a,b) for  $R_{nk}$  and representing products in terms of partial fractions (Paul, 1973, p. 417, 418) leads to

$$\begin{aligned}
s_n &= \frac{n(n+1)}{(2n+1)(n-1)(n+2)} \left\{ P_n \rho \sum_{\substack{k=1 \\ k \neq n-1}}^{\infty} P_k \left| \frac{2(2n+1)}{n(n+1)} \frac{1}{k} - \frac{n+2}{k-(n-1)} - \frac{n-1}{k+n+2} \right| \right. \\
&\quad \cdot \rho^{k+1} + \left( P_{n+1} - P_{n-1} \right) \sum_{\substack{k=2 \\ k \neq n}}^{\infty} P_k \rho^{k+1} \left| \frac{3}{k-1} - \frac{n+2}{k-n} + \frac{n-1}{k+n+1} \right| \\
&\quad - P_n \frac{1}{\rho} \sum_{\substack{k=3 \\ k \neq n+1}}^{\infty} P_k \rho^{k+1} \left| \frac{2(2n+1)}{n(n+1)} \frac{1}{k+2} - \frac{n+2}{k-(n+1)} - \frac{n-1}{k+n} \right| \Big\} \\
&\quad + \frac{2n+1}{n-1} \rho^{n+1} R_{nn} . \tag{4.37}
\end{aligned}$$

All occurring infinite sums have already been used before and can be found in Table 4.1 ; the corresponding closed expressions are given in equations (4.26a,b,c). Introducing them in (4.37), leads to the explicit form of the eigenvalue,

$$\begin{aligned}
s_n(\rho, t_0) &= \frac{n(n+1)}{(2n+1)(n-1)(n+2)} \left\{ \left( P_{n+1} - P_{n-1} \right) \left| 3 \left( F_{-1} - \frac{1}{n-1} \right. \right. \right. \\
&\quad \cdot \rho^{n+1} P_n \Big) - (n+2) \left( \rho^{n+1} U_{n+1} + \frac{\rho}{n} + \frac{\rho^2 P_1}{n-1} \right) + (n-1) \cdot \\
&\quad \cdot \left( F_{n+1} - \frac{\rho}{n+1} - \frac{\rho^2}{n+2} P_1 - \frac{\rho^{n+1}}{2n+1} P_n \right) + \frac{2(2n+1)}{n(n+1)(n-1)} \cdot \\
&\quad \cdot \rho^{n+1} P_n - \frac{n-1}{2n+1} \rho^{n+1} P_n \Big| + P_n \left\{ - (n-1) \left| \rho F_{n+2} - \frac{1}{\rho} F_n \right. \right. \\
&\quad + \frac{\rho^2}{n+2} \left( P_2 - P_0 \right) + \frac{1}{n} + \frac{\rho}{n+1} P_1 \Big| + (n+2) \left| \rho^{n+1} \left( U_{n+2} - U_n \right) \right. \right. \\
&\quad + \frac{\rho^2}{n-1} \left( P_2 - P_0 \right) + \frac{1}{n+1} + \frac{\rho P_1}{n} \Big| + \frac{2(2n+1)}{n(n+1)} \left| \rho F_0 - \frac{1}{\rho} F_{-2} \right| \Big\} \\
&\quad + \frac{2n+1}{n-1} \rho^{n+1} R_{nn} . \tag{4.38}
\end{aligned}$$

The eigenvalues have to fulfil the following conditions:

a)  $s_n(\rho, -1) \equiv 0$  because of coinciding limits of integration,

b)  $s_n(\rho, 1) = \frac{2}{n-1} \rho^{n+1}$  for  $n \geq 2$ ; this follows from the orthogonality of the Legendre polynomials.

As a matter of fact  $s_n(1, t_0)$  equals the Molodensky coefficient  $Q_n$  defined before,

$$s_n(1, t_0) = Q_n(t_0).$$

Let the gravity anomalies  $f$  be expanded into a series of Laplace surface harmonics,

$$f(P_0) = \sum_n f_n(P_0);$$

then we know from (4.6) that the disturbing potential at the level of  $P$  can simply be obtained through a multiplication of the Laplace surface harmonics by the eigenvalues which relate both quantities; it follows from (4.1a) that

$$T(P) = \frac{R}{2} \sum_n s_n(\rho, 1) f_n(P). \quad (4.39)$$

If gravity information is neglected outside a cap of radius  $\psi = \psi_0$  around the computation point  $P$ , an error is committed which can be calculated by simply replacing the eigenvalue  $s_n(\rho, 1)$  by the eigenvalue of the corresponding truncated kernel  $s_n(\rho, t_0)$ ,

$$e_T(P) = \frac{R}{2} \sum_n s_n(\rho, t_0) f_n(P).$$

Following identical arguments as in the case of the radial derivative of  $T$ , and using the same notation  $s_n$  for the eigenvalues of the moving average kernel, we obtain a total representation error in

the disturbing potential,

$$e_T(P) = \frac{R}{2} \sum_n \sum_{i=1}^I s_n(\rho, t_{i-1}) [\beta(\tau_{i-1}) - \beta(\tau_i)] f_n(P) \quad (4.40)$$

with  $s_n(\tau_0) = s_n(1) \equiv 1$  and  $t_0 = 1$ ;  $I$  stands for the number of regions. With

$$\lambda_n := \frac{\rho}{2} \sum_{i=1}^I s_n(\rho, t_{i-1}) [\beta(\tau_{i-1}) - \beta(\tau_i)] \quad (4.41)$$

equation (4.40) reduces to

$$e_T(P) = r \sum_n \lambda_n f_n(P) . \quad (4.42)$$

At this point we turn from the disturbing potential to the horizontal components of its gradient,  $\frac{1}{r_p} D_\phi T$  and  $\frac{1}{r_p \cos \phi} D_\lambda T$ ; the gravity anomaly representation error has an impact onto these two quantities which can directly be derived from (4.42) :

$$e_{\delta_\phi}(P) = \sum_n \lambda_n D_\phi f_n \quad (4.43)$$

and

$$e_{\delta_\lambda}(P) = \frac{1}{\cos \phi} \sum_n \lambda_n D_\lambda f_n .$$

The mean square error of the total horizontal component

$$m_\theta^2 = M \left\{ e_{\delta_\phi}^2 + e_{\delta_\lambda}^2 \right\}$$

is thus given by

$$m_\theta^2 = \sum_n \sum_{n'} \lambda_n \lambda_{n'} M \left\{ D_\phi f_n(P) D_\phi f_{n'}(P) + \frac{1}{\cos^2 \phi} D_\lambda f_n(P) D_\lambda f_{n'}(P) \right\},$$

which, according to (Heiskanen and Moritz, 1967, p. 262), reduces to

$$m_\theta^2 = \sum_{n=2}^{\infty} \lambda_n^2 n(n+1) c_n \quad (4.44)$$

with the degree variances defined in (4.33).

Equations (4.35) and (4.44) are the desired representation error estimates for the radial and the total horizontal component of the disturbing potential's gradient.

#### 4.2 Estimation of the error due to data inaccuracy.

In the foregoing section the error has been estimated which resulted from a replacement of the (unknown) actual gravity anomaly function by mean values with variable block size depending on its distance from the computation point (see Table 2.1); in order to obtain manageable expressions, the mean value representation was formally replaced by a corresponding moving average. The estimated error has been called representation error.

In general, the mean gravity anomalies are affected by noise which primarily stems from the mean value estimation process. This noise is the second important error source. Its impact on the gradient of the disturbing potential could be calculated if the error covariance function would be known; this, however, is hardly

ever the case. Under such circumstances, it is a widely applied practice to consider the anomaly estimates as independent.

Performing the horizontal differentiations in (4.2), we obtain the gradient of  $T$  in the following form (Heiskanen and Moritz, 1967, pp. 233, 234)

$$\delta_r(P) = \frac{R}{4\pi} \iint_{\sigma} D_{r_p} S(P, Q) \Delta g(Q) d\sigma(Q) ,$$

$$\delta_\phi(P) = - \frac{R}{4\pi r_p} \iint_{\sigma} D_{\psi_{PQ}} S(P, Q) \cos \alpha_{PQ} \Delta g(Q) d\sigma(Q) \quad (4.2)'$$

$$\delta_\lambda(P) = - \frac{R}{4\pi r_p} \iint_{\sigma} D_{\psi_{PQ}} S(P, Q) \sin \alpha_{PQ} \Delta g(Q) d\sigma(Q) .$$

According to the individual block sizes of the mean values, the integral has to be splitted up into  $J$  subintegrals if  $J$  mean anomalies are to be considered for the estimation of the grad  $T$ . Denoting the rms estimate of the  $j$ 'th mean anomaly's error by  $m_j$ , its propagation into the components of grad  $T$  is as follows

$$\bar{m}_{\delta_r}^2(P) = \left( \frac{R}{4\pi} \right)^2 \sum_{j=1}^J m_j^2 \left[ \iint_{\sigma_j} D_{r_p} S(P, Q) d\sigma(Q) \right]^2 ,$$

$$\bar{m}_{\delta_\phi}^2(P) = \left( \frac{R}{4\pi r_p} \right)^2 \sum_{j=1}^J m_j^2 \left[ \iint_{\sigma_j} D_{\psi_{PQ}} S(P, Q) \cos \alpha_{PQ} d\sigma(Q) \right]^2 , \quad (4.45)$$

$$\bar{m}_{\delta_\lambda}^2(P) = \left( \frac{R}{4\pi r_p} \right)^2 \sum_{j=1}^J m_j^2 \left[ \iint_{\sigma_j} D_{\psi_{PQ}} S(P, Q) \sin \alpha_{PQ} d\sigma(Q) \right]^2 .$$

The integrals can be evaluated using a fast numerical integration procedure described in (Sünkel and Rummel, 1981).

## 5. COLLOCATION VERSUS INTEGRAL APPROACH

Two methods of gravity disturbance vector estimation have been presented here, the least-squares collocation solution and the integral solution. Although they seem to be totally different, they share a number of common features.

Let us begin with the data:

The accuracy of the three components of the gravity disturbance vector is estimated on the basis of mean free air gravity anomalies; mean anomalies are defined on "rectangular" blocks bounded by meridians and parallels, therefore, they are bound to the global coordinate system; the operator which can be thought of transforming the actual gravity anomaly function into its mean value representation is non-isotropic.

Covariance functions, which are commonly in use, are isotropic; kernels of integral formulas are also mainly isotropic. Anisotropy causes problems with the integration of covariance functions and with the integration of integral kernels. In order to avoid these difficulties, isotropy is artificially produced through a replacement of the mean value concept by the concept of moving average over a circular region. Both collocation and integral formulae (representation error estimation) use the eigenvalues  $\beta_n$  of the moving average kernel; in the estimation of the representation error, the eigenvalues are used explicitly, in least-squares collocation, they enter implicitly via the covariance function. (Usually, an approximation is used in order to obtain closed covariance expressions.)

The data error estimates enter in collocation through the error covariance matrix, which has diagonal form if no correlations are assumed; the same diagonal form has been assumed for the estimation of the error due to data inaccuracy.

As far as the use of statistical gravity field information is concerned, there is also no difference between the two methods: both use this information in terms of a degree variance model (and empirical degree variances for lower degrees); again, it enters into collocation implicitly via the covariance function and appears explicitly in the representation error estimation equation.

The upward continuation is contained in the eigenvalues of the kernel (representation error) and implicitly in the individual covariances (collocation).

If no data are available, both methods provide identical error estimates; if the gravity anomaly would be known at every point of the sphere, the collocation solution would again coincide with the integral solution. For these reasons, we can expect that the estimations will differ only little if the gravity coverage is reasonably good - a fact which was strongly confirmed by numerical calculations.

## 6. RESULTS - CONCLUSIONS

The error estimations of the radial and horizontal components which are presented here, have been carried out by least-squares collocation and / or integral formula approach. The deviation was found to be in the 10% range and less, dependent mainly on the data distribution; therefore, the results presented here are practically valid for both methods.

The numerical investigation was started with a small data set consisting of 5' x 5' mean anomalies around the computation point; between 4 and 144 anomalies have been considered for the estimation; two cases have been studied: error-free anomalies and anomalies with a rms-error of  $\pm 8$  mgal; the prediction point's latitude was assumed to be zero; Tscherning's degree variance model 2 has been used with 36 lower harmonics subtracted; this corresponds quite well to the assumption of error-free  $5^\circ \times 5^\circ$  anomalies given outside the small region in which 5' x 5' anomalies are available. Of course, this is a rather poor data distribution and is not representative for the available distribution; I, however, like to present the result because it shows the essential behavior of all solutions remarkably well:

### Radial component:

- a) The error decreases rapidly if the number of 5' x 5' mean anomalies around the computation point increases;
- b) the larger the 5' x 5' data set, the smaller is the representation error (evident);
- c) the influence of data errors decreases with increasing altitude;
- d) a very typical feature is the cone-effect: the data region of strong contribution increases with increasing prediction height, or with other words, if the number of anomalies is

kept constant, the prediction error increases with increasing altitude.

Horizontal component:

- a) for the same data constellation, the error is more than twice as high and decreases only relatively slowly, if the number of 5' x 5' anomalies increases;
- b) the larger the data set, the smaller is the representation error (evident);
- c) the influence of data errors decreases with increasing altitude;
- d) the remote zones have a very significant influence on the result (this is also known from the behavior of gravimetrically determined deflections of the vertical, which are very closely related to the horizontal components of grad T).

LEAST-SQUARES COLLOCATION PREDICTED ERROR ESTIMATES  
 FOR GRAVITY DISTURBANCES IN HIGH ALTITUDE (RADIAL COMPONENT)  
 \* 1 ... 4 BLOCKS OF 5' BY 5' MEAN ANOMALIES  
 \* 2 ... 16 BLOCKS OF 5' BY 5' MEAN ANOMALIES  
 \* 3 ... 64 BLOCKS OF 5' BY 5' MEAN ANOMALIES  
 \* 4 ... 144 BLOCKS OF 5' BY 5' MEAN ANOMALIES  
 MEAN ANOMALY STANDARD ERROR : 0 MGAL RMS, 8 MGAL RMS  
 COVARIANCE FUNCTION PARAMETERS USED : S=0.999617, R=425.28.  
 MODEL T2, 36 LOWER HARMONICS SUBTRACTED  
 RMS ERROR ESTIMATES ARE IN MGAL

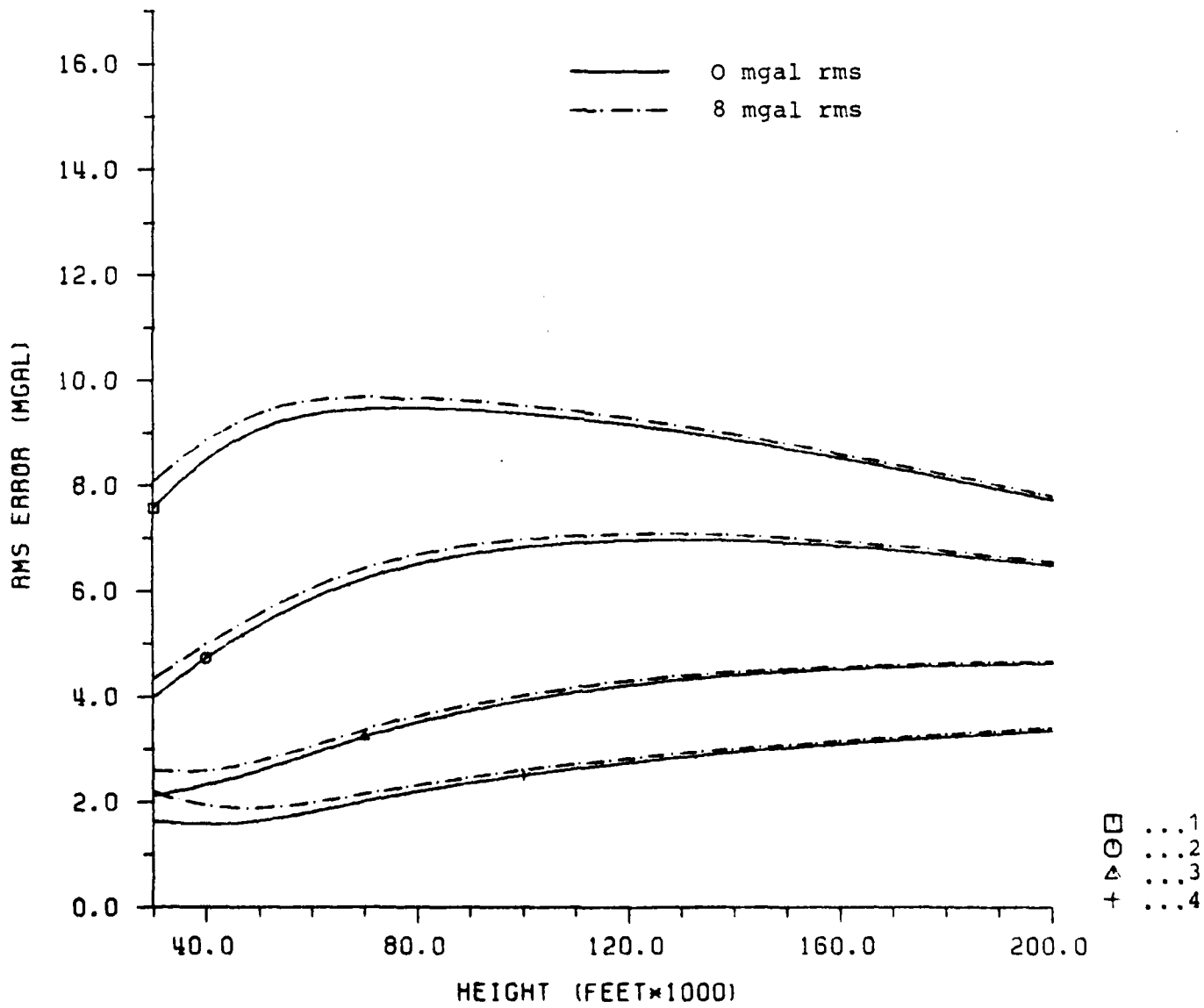


Fig. 6.1a Prediction error estimation test

LEAST-SQUARES COLLOCATION PREDICTED ERROR ESTIMATES  
 FOR GRAVITY DISTURBANCES IN HIGH ALTITUDE (HORIZONTAL COMPONENT)  
 \* 1 ... 4 BLOCKS OF 5' BY 5' MEAN ANOMALIES  
 \* 2 ... 16 BLOCKS OF 5' BY 5' MEAN ANOMALIES  
 \* 3 ... 64 BLOCKS OF 5' BY 5' MEAN ANOMALIES  
 \* 4 ... 144 BLOCKS OF 5' BY 5' MEAN ANOMALIES  
 MEAN ANOMALY STANDARD ERROR : 0 MGAL RMS, 8 MGAL RMS  
 COVARIANCE FUNCTION PARAMETERS USED : S=0.999617, A=425.28,  
 MODEL T2, 36 LOWER HARMONICS SUBTRACTED  
 RMS ERROR ESTIMATES ARE IN MGAL

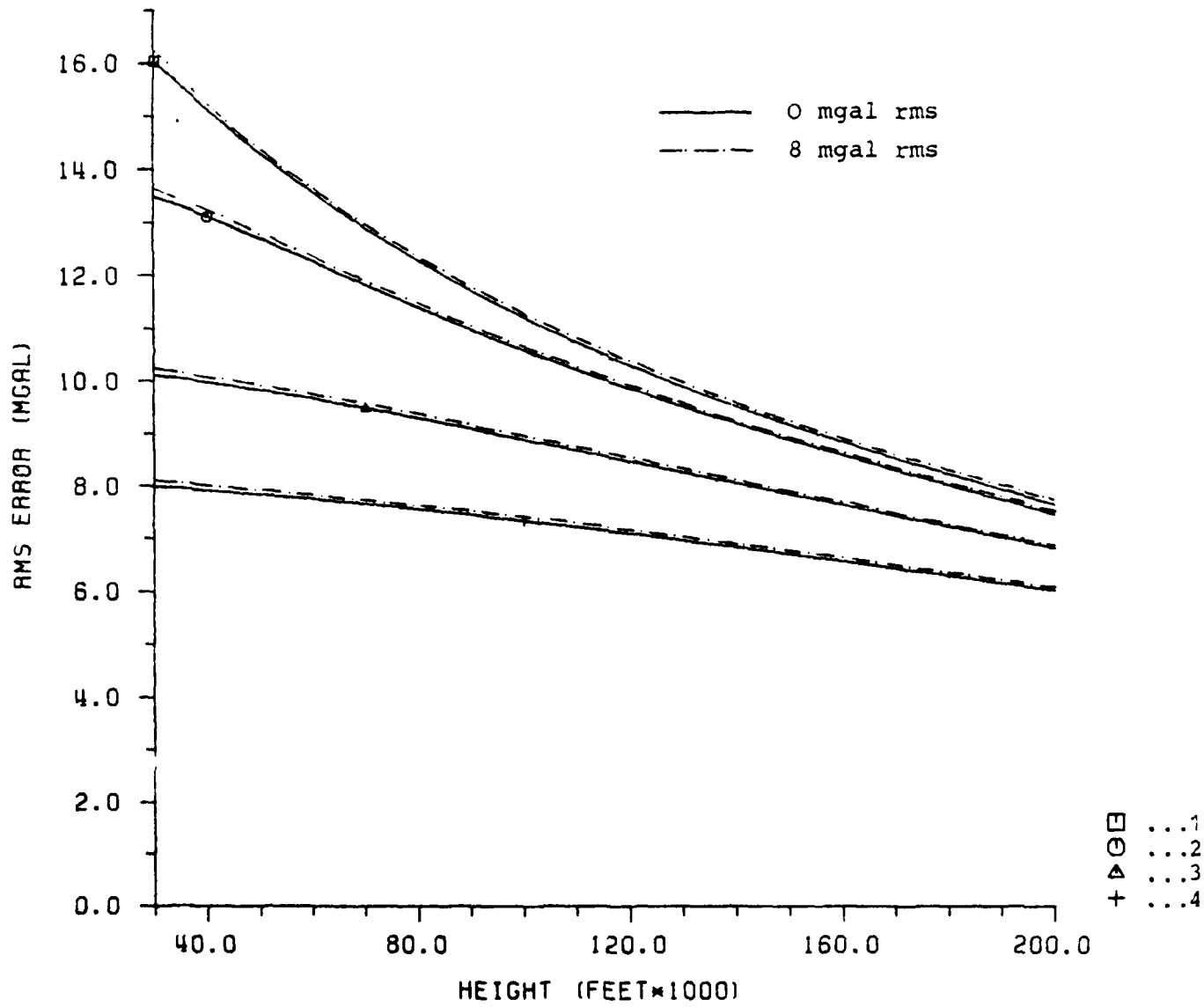


Fig. 6.1b Prediction error estimation test

Table 6.1 contains the error estimates which have been obtained using the data set described in Table 2.1 with data error estimates presented in Table 2.2. From these figures, we can draw the following conclusions:

- a) For a fixed altitude, the different kinds of data distribution (case 1 to 9) produce no significant variation in the estimation of the radial component; the horizontal component estimates differ from case to case up to 50%.
- b) The rms-estimates for the radial component are strongly influenced by the data inaccuracy which accounts for up to 90% of the total error in low altitudes; the data error impact on the radial component decreases rapidly with increasing elevation. Error-free data give estimates in  $\delta_r$  of  $\pm 0.4$  mgal for 30 000 ft down to  $\pm 0.07$  mgal for 200 000 ft altitude; these figures are in excellent agreement with the ones derived from the representation error formula.

With the available data (distribution, rms-errors), the radial component of the gravity disturbance vector can be estimated with a rms-error of  $\pm 1$  mgal at an altitude of about 50 000 feet. In order to achieve the same accuracy in 30 000 ft elevation, the data inaccuracy has to be reduced by about 60%, particularly in the region around the computation point (5' x 5' anomalies); remote zones contribute only little.

- c) The situation looks much worse for the horizontal components: compared to the radial component, they are more inaccurate from a factor 2 (at 30 000 feet altitude) up to a factor 6 (at 200 000 feet altitude); the impact of data inaccuracies is relatively little (between  $\pm 1.1$  mgal (30 000 feet) and  $\pm 0.2$  mgal (200 000 feet)); the crucial point is the data distribution : the representation error varies between  $\pm 0.2$  mgal (case 9) and  $\pm 2.9$  mgal (case 1) and decreases very slowly with increasing elevation (less than 10% in the range from 30 000 to 200 000 feet).

With the available data (distribution, rms-errors), the

horizontal components of the gravity disturbance vector can be estimated with an accuracy of  $\pm 2.3$  mgal at 30 000 ft elevation with the best data distribution available (case 9a); this corresponds to an accuracy of  $\pm 0.^{\circ}5$  for the direction of the gravity vector. An improvement to  $\pm 1$  mgal ( $\pm 0.^{\circ}2$ ) at 30 000 ft altitude requires a considerably better representation of the gravity anomaly field; unlike in the case of the radial component, the horizontal component responds also considerably to the representation in the medium range (up to  $30^{\circ}$  spherical distance from the computation point). In this critical region the block sizes need to be reduced by a factor of about 2 and the overall data accuracy should be increased by about 30% in order to achieve this goal.

case	30 000 ft		40 000 ft		70 000 ft		100 000 ft		200 000 ft	
	radial	hor.	radial	hor.	radial	hor.	radial	hor.	radial	hor.
1a	±1.5	±3.1	±1.2	±3.0	±0.7	±2.9	±0.6	±2.9	±0.4	±2.8
b	±1.8	±3.2	±1.4	±3.1	±0.9	±2.9	±0.7	±2.9	±0.5	±2.8
2a	±1.5	±3.0	±1.2	±2.9	±0.7	±2.8	±0.6	±2.7	±0.4	±2.6
b	±1.8	±3.1	±1.4	±2.9	±0.9	±2.8	±0.7	±2.7	±0.5	±2.6
3a	±1.5	±2.8	±1.2	±2.7	±0.7	±2.6	±0.6	±2.6	±0.4	±2.5
b	±1.8	±2.9	±1.4	±2.8	±0.9	±2.6	±0.7	±2.6	±0.5	±2.5
4a	±1.5	±2.6	±1.2	±2.5	±0.7	±2.4	±0.6	±2.4	±0.4	±2.3
b	±1.8	±2.8	±1.4	±2.6	±0.9	±2.4	±0.7	±2.4	±0.5	±2.3
5a	±1.5	±2.8	±1.2	±2.7	±0.7	±2.6	±0.6	±2.6	±0.4	±2.5
b	±1.8	±2.9	±1.4	±2.8	±0.9	±2.6	±0.7	±2.6	±0.5	±2.5
6a	±1.5	±2.7	±1.2	±2.6	±0.7	±2.5	±0.6	±2.4	±0.4	±2.3
b	±1.8	±2.8	±1.4	±2.6	±0.9	±2.5	±0.7	±2.4	±0.5	±2.3
7a	±1.5	±2.7	±1.2	±2.6	±0.7	±2.5	±0.6	±2.5	±0.4	±2.4
b	±1.8	±2.8	±1.4	±2.7	±0.9	±2.5	±0.7	±2.5	±0.5	±2.4
8a	±1.5	±3.0	±1.1	±2.9	±0.7	±2.8	±0.6	±2.7	±0.4	±2.6
b	±1.8	±3.1	±1.4	±2.9	±0.9	±2.8	±0.7	±2.7	±0.4	±2.6
9a	±1.5	±2.3	±1.1	±2.2	±0.7	±2.1	±0.6	±2.0	±0.4	±1.9
b	±1.8	±2.4	±1.4	±2.2	±0.8	±2.1	±0.6	±2.0	±0.4	±1.9

TABLE 6.1 rms-error estimates of gravity disturbance  
vector components in various altitudes  
(dimension: mgal )

**ACKNOWLEDGEMENTS**

The author expresses his appreciation to Prof. Dr. H. Moritz for discussions and constructive comments. Computer time has been made available by the Instruction and Research Computer Center of the Ohio State University and the *EDV-Zentrum Graz*.

**KEY WORDS**

disturbing potential  
least-squares collocation  
integral formula  
isotropic integral kernel  
frequency domain

## REFERENCES

Colombo, O.L. (1979) : Optimal estimation from data regularly sampled on a sphere with applications in geodesy.  
Report No. 291, Department of Geodetic Science, The Ohio State University, Columbus, Ohio.

Heiskanen, W.A. and H. Moritz (1967) : Physical Geodesy.  
Freeman & Co., San Francisco.

Meissl, P. (1971a) : A study of covariance functions related to the earth's disturbing potential.  
Report No. 151, Department of Geodetic Science, The Ohio State University, Columbus, Ohio.

Meissl, P. (1971b) : Preparations for the numerical evaluation of second order Molodensky-type formulas.  
Report No. 163, Department of Geodetic Science, The Ohio State University, Columbus, Ohio.

Moritz, H. (1980) : Advanced Physical Geodesy.  
Wichmann Verlag, Karlsruhe.

Müller, C. (1966) : Spherical harmonics.  
Lecture Notes in Mathematics, No. 17, Springer-Verlag, Berlin.

Paul, M.K. (1973) : A method of evaluating the truncation error coefficients for geoidal height.  
Bulletin Géodésique, No. 110, pp. 413 - 425.

Rapp, R.H. and S.T. Agajelu (1975) : Comparison of upward continued anomalies computed by the Poisson integral and by collocation.

Report No. 227, Department of Geodetic Science, The Ohio State University, Columbus, Ohio.

Schwarz, K.P. (1976) : Geodetic accuracies obtainable from measurements of first and second order gravitational gradients.

Report No. 242, Department of Geodetic Science, The Ohio State University, Columbus, Ohio.

Sünkel, H. (1978) : Approximation of covariance functions by non-positive definite functions.

Report No. 271, Department of Geodetic Science, The Ohio State University, Columbus, Ohio.

Sünkel, H. (1980) : A general surface representation module designed for geodesy.

Report No. 292, Department of Geodetic Science, The Ohio State University, Columbus, Ohio.

Sünkel, H. and R. Rummel (1981) : On the numerical evaluation of spherical integral formulas based on mean values.

Bulletino di Geodesia e Scienze Affini, (in print).

Tscherning, C.C. (1972) : Representation of covariance functions related to the anomalous potential of the earth using reproducing kernels.

Internal Report No. 3, Danish Geodetic Institute, Copenhagen.

Tscherning, C.C. and R.H. Rapp (1974) : Closed covariance expressions for gravity anomalies, geoid undulations, and deflections of the vertical implied by anomaly degree variance models.

Report No. 208, Department of Geodetic Science, The Ohio State University, Columbus, Ohio.

Tscherning, C.C. (1976) : Covariance expressions for second and lower order derivatives of the anomalous potential.

Report No. 225, Department of Geodetic Science, The Ohio State University, Columbus, Ohio.

Zurmühl, R. (1964) : Matrizen und ihre technischen Anwendungen.  
Springer-Verlag, Berlin.

